

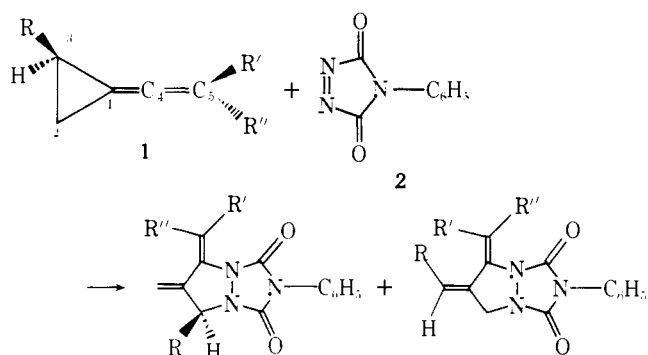
Reinterpretation of the Mechanisms of Concerted Cycloaddition and Cyclodimerization of Allenes

Daniel J. Pasto

Contribution from the Department of Chemistry, University of Notre Dame, Notre Dame, Indiana 46556. Received March 3, 1978

Abstract: The cycloaddition and cyclodimerization reactions of allenes have been evaluated in terms of a concerted $[\pi 2_s + (\pi 2_s + \pi 2_s)]$ mechanism in which the dienophile interacts with one p AO of each double bond of the allene, the exocyclic double bond of the product being formed from the two remaining orthogonal p AO's by rotation of the terminal allene methylene group. The application of second-order PMO theory to this process results in predictions of chemo-, regio-, and stereoselectivities consistent with experimental observations. Similar calculations on the $(\pi 2_s + \pi 2_a)$ process predict no definite situ- or regioselectivities should be observed and result in incorrect predictions in a couple of cases.

Recent studies in our laboratories have involved a detailed analysis of the cycloaddition reactions of alkenylidenecyclopropanes (**1**) with 4-phenyl-1,2,4-triazoline-3,5-dione (**2**).¹

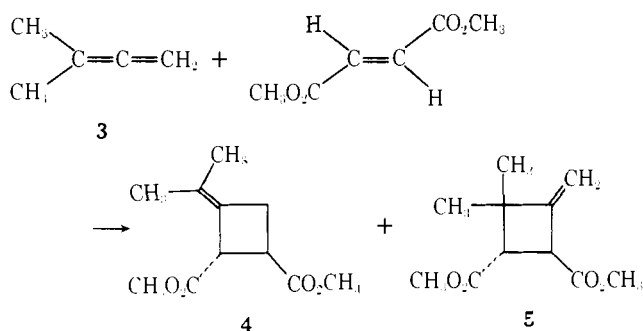


Stereochemical² and kinetic³ studies of the reactions of **1** with **2** and comparisons with the reactions of **1** with dipolar-⁴ and diradical-intermediate⁵ reagents, and the reactions of methylenecyclopropanes⁶ and vinylcyclopropanes,⁷ with **1**, provided support for a concerted cycloaddition process. Theoretical studies⁸ led to a clarification of the bonding interactions in **1** and in the transition state for concerted cycloaddition. The atomic orbital interactions involved in the cycloaddition process are shown in Figure 1, along with the indicated directions of rotation of R-C₃-H and R'-C₅-R'' planes. The AO interactions in the transition state represent a "Möbius aromatic transition state" in terms of the Hückel-Möbius concept of chemical reactivity.⁹

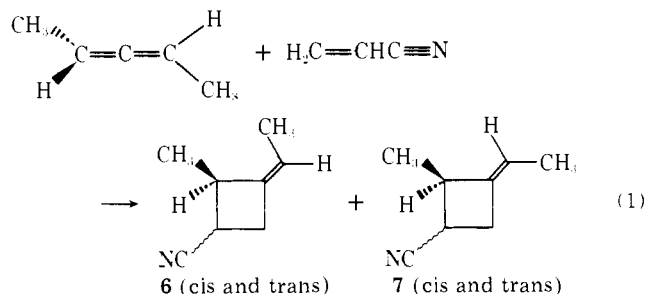
The cycloaddition of **1** (R = C₆H₅, R' = R'' = CH₃) with **2** occurs with great facility ($\Delta H^\ddagger = 9.6 \pm 1.5$ kcal/mol, $\Delta S^\ddagger = -23 \pm 3$ eu)³ despite the fact that two orthogonal relationships exist between AO's in the reactant which must ultimately form the two π systems in the product. This necessitates the two 90° rotations shown in Figure 1. Such orthogonal relationships between AO's in a reactant would in general be considered to result in prohibitively high activation barriers; however, in the case of the reaction of **1** with **2** this is obviously not true. Accordingly, a search was undertaken to discover other reactions in which AO's that are orthogonal in the starting state interact in the transition state leading to bond formation in the final product. Initial attention has been focused on reactions of allenes, i.e., cycloaddition and cyclodimerization reactions of allenes and hydrogen [1,3]-sigmatropic rearrangements. In the present paper an alternative to the $(\pi 2_s + \pi 2_a)$ concerted process is described.

Considerable attention has been devoted to the study of the cycloaddition reactions of allenes with alkenes and the cyclodimerization of allenes. In cycloaddition reactions of allenes with substituted alkenes stereochemistry is retained about both

the allene and alkene portions. The cycloaddition of 1,1-dimethylallene (**3**) with dimethyl fumarate is reported to produce the two adducts **4** and **5** in a 11.5:1 ratio in which >99% ste-



reoselectivity is claimed.¹⁰ The reaction of optically active 2,3-pentadiene with acrylonitrile is reported to give four stereoisomeric adducts, all of which are optically active.¹¹ Despite these seemingly stereochemically concordant results, different mechanisms have been proposed: in the former, a concerted $(\pi 2_s + \pi 2_a)$ process was proposed;¹⁰ in the latter, a two-step, diradical intermediate mechanism was proposed.¹¹



An interesting aspect of the cycloadditions of allenes is that of the chemoselectivity in the cycloadditions of alkyl substituted allenes. 1,2-Pentadiene is reported to react with maleic anhydride to produce **8** and **9** in 25 and 52% yields, respectively, while reaction of **3** with maleic anhydride produces only **10**.¹² The reasons for the observed chemoselectivity have not been discussed.

Hydrogen-deuterium isotope effects have been measured in cycloaddition reactions of 1,1-dideuterioallene with two-, three-, and four-electron components.¹³ It was concluded that allenes undergo concerted (3 + 2) and (4 + 2) cycloadditions and nonconcerted (2 + 2) cycloadditions, and that "allene reacts like a reasonably normal alkene in its cycloadditions".¹³

The regioselectivity in the cycloaddition of allene with acrylonitrile has been interpreted in terms of a diradical inter-

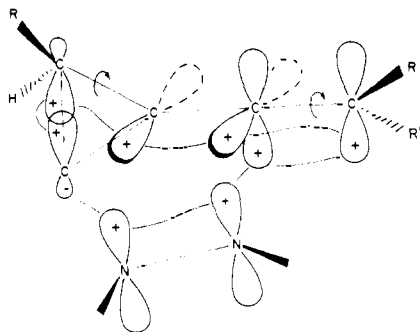
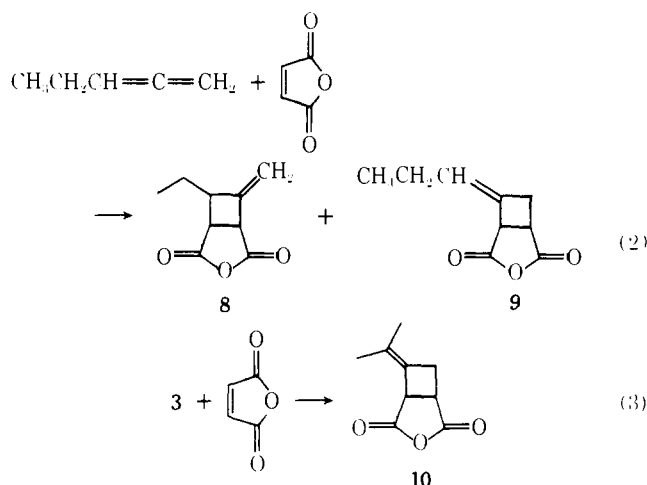
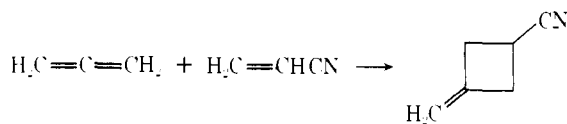


Figure 1. Orbital interactions in the transition state for cycloaddition of **1** with **2**. (The arrows indicate the direction of rotation of the H-C-R and R-C-R' groups.)



mediate mechanism; however, as will be shown later in this paper the regioselectivity is also consistent with a concerted process.

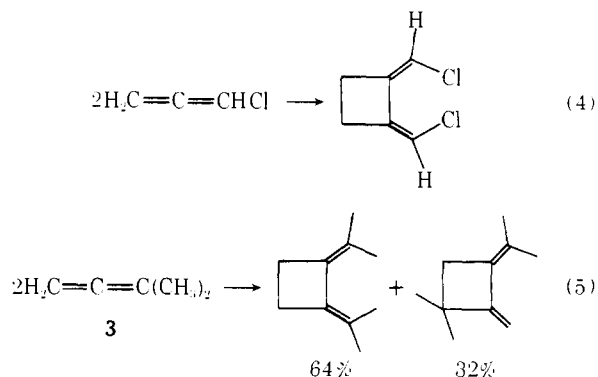


The conclusion that allene reacts like a reasonably normal electron-rich alkene in concerted cycloadditions is not supported by either spectroscopic or chemical reactivity data. Spectroscopically, a C=C of allene is essentially identical with the C=C of ethene. Allene possesses an absorption maximum at 1710 Å tailing off near 2030 Å,¹⁴ while ethene displays a flat maximum at 1750 Å.¹⁵ Allene displays photoelectron spectroscopic (PES) ionization potentials (IP) at 10.07 and 10.64 eV¹⁶ (Jahn-Teller splitting), while the PES IP of ethene is 10.51.¹⁷ Orbital energies calculated by the 4-31G ab initio method^{18,19} for allene and ethene are very similar: for allene $E_{\text{HOMO}} = -10.1326$ eV and $E_{\text{LUMO}} = 5.0141$ eV (both degenerate); for ethene $E_{\text{HOMO}} = -10.1896$ eV and $E_{\text{LUMO}} = 5.0451$ eV. Despite their spectroscopic similarity, allenes and alkenes are *not* similar in chemical reactivity toward cycloaddition. Allenes are tremendously more reactive toward cycloaddition. For example, methylallene undergoes 68% reaction at 170 °C in 13 h,²⁰ but ethene and propene show no tendency whatever to undergo cycloaddition under these reaction conditions, or for that matter, under much more strenuous reaction conditions. It is this tremendous difference in reactivity despite very similar molecular orbital (MO) (electronic) properties that particular attention will be focused on in this paper.

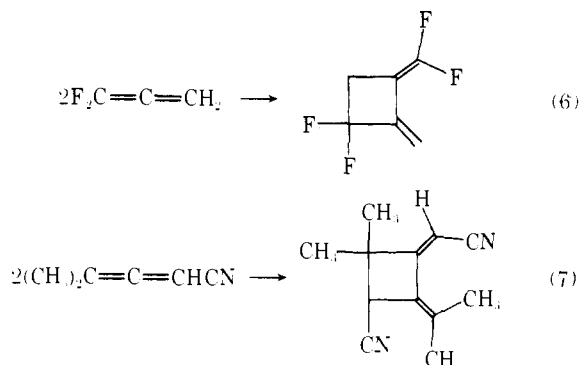
The mechanism of the cyclodimerization of allenes is also in a state of debate, with some of the same evidence being in-

terpreted differently by different authors. Optically active 1,2-cyclononadiene and 2,3-pentadiene cyclodimerize to produce optically active products; 1,2-cyclononadiene cyclodimerizes with an estimated 100% stereoselectivity leading the authors to suggest that the reaction occurs via a concerted $\pi 2_s + \pi 2_a$ process, although a restricted diradical process could not be ruled out.²¹ In the paper on the 2,3-pentadiene cyclodimerization it was noted that the results were consistent with, but not demanding of, a concerted ($\pi 2_s + \pi 2_a$) process, and that a restricted diradical-intermediate mechanism, or perhaps even some other mechanistic alternative, might be operative.²²

The regioselectivities in allene cyclodimerizations depend on the nature of the function(s) attached to the allene chromophore. Chloroallene²³ and 3²⁴ dimerize predominantly in



a head-to-head manner, whereas difluoroallene²⁵ and 3,3-dimethyl-1-cyanoallene²⁶ dimerize in a head-to-tail manner. These results are not readily rationalized on the basis of either a ($\pi 2_s + \pi 2_a$) concerted or a nonconcerted process.



Another interesting stereochemical feature in the cyclodimerization of substituted allenes is the stereochemistry about the exocyclic double bond in the product. In the cyclodimerization of **14** and **16** as well as in many other cyclodimerizations not discussed herein, the functions attached to the exocyclic double bond in the product are directed toward the inside of the diene chromophore in the most sterically congested position. This feature of the cyclodimerization of allenes has not been previously adequately rationalized.^{22,23}

The hydrogen-deuterium isotope effect in the cyclodimerization of 1,1-dideuterioallene also has been measured and, on the basis of comparison the H-D isotope effects observed in (3 + 2) and (4 + 2) cycloaddition processes, has been interpreted in terms of a multistep, diradical intermediate mechanism.¹³

In view of the unresolved controversy over the mechanisms of the cycloaddition and cyclodimerization reactions of allenes, second-order perturbation molecular orbital theory²⁷ (PMO) has been applied to these reactions in order to evaluate the relative interaction energies (E_{int}) of the various modes of concerted cycloaddition. In the following sections of this paper the results of such calculations on the cycloaddition and cy-

clodimerization of allenes are reported and the predicted and experimentally observed regioselectivities are compared. These calculations do not provide insight on the aspect of concerted vs. nonconcerted cycloaddition mechanisms.

Results and Discussion

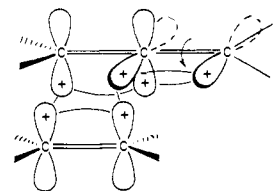
Transition State Models for Allowed, Concerted Cycloadditions. Two transition-state models for allowed, concerted cycloadditions of allenes are evaluated: the first being the previously considered $(\pi 2_s + \pi 2_s)$ process, the second being $[\pi 2_s + (\pi 2_s + \pi 2_s)]$ processes²⁸ (see Figure 2) in which one p orbital of the dienophile interacts with a p orbital of one C=C of the allene in a coaxial manner with the other p orbital of the dienophile interacting with a p orbital of the other C=C of the allene in a perpendicular manner. In this latter process the exocyclic double bond in the product is derived from the remaining p orbitals of the two double bonds, which are orthogonal in the reacting state, necessitating a 90° rotation of the penultimate methylene. The direction of rotation will be to achieve the greater stabilization afforded in a Hückel "aromatic"¹⁹ transition state as illustrated in Figure 2. (The stereochemical consequences of this will be discussed in a later section.) Two structurally different transition states are possible for this type of process: one involving coaxial overlap of a p orbital on a terminal carbon of the allene, the other involving coaxial overlap with a p orbital on the central carbon of the allene.

Calculation of Interaction Energies. Interaction energies in the transition states have been calculated using second-order PMO theory²⁷ according to

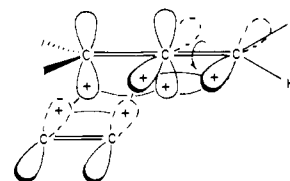
$$E_{int} = - \sum_{rr'} (q_r + q_{r'}) \eta_{rr'} S_{rr'} - 2 \sum_j^{occ} \sum_{k'}^{unocc} \left[\frac{\left(\sum_{rr'} c_{jr} c_{k'r'} \eta_{rr'} \right)^2}{E_{k'} - E_j} + \frac{1}{4} (E_{k'} - E_j) \left(\sum_{rr'} c_{jr} c_{k'r'} S_{rr'} \right)^2 \right] - 2 \sum_{j'}^{occ} \sum_{k}^{unocc} \left[\frac{\left(\sum_{rr'} c_{k'r} c_{j'r'} \eta_{rr'} \right)^2}{E_k - E_{j'}} + \frac{1}{4} (E_k - E_{j'}) \left(\sum_{rr'} c_{k'r} c_{j'r'} S_{rr'} \right)^2 \right] + \sum_{rr'} \Delta q_r \Delta q_{r'} / R_{rr'} \quad (8)$$

in which q is the total electron density on the interacting atoms r and r' of the two reactants, Δq is the net charge, c 's are coefficients of the AO's in the k and j ground-state MO wave functions of the reactants, $S_{rr'}$ is the overlap integral for the interacting AO's, $\eta_{rr'}$ is the overlap energy integral (which is proportional to $S_{rr'}$, i.e., $\eta_{rr'} = k S_{rr'}$), and $R_{rr'}$ is the distance between atoms r and r' . The first term is the closed shell repulsion energy contribution, the second and third are the attractive overlap energy contributions, while the fourth is the polar (electrostatic) energy contribution term.

Ground-state MO wave functions for the molecules included in this study have been calculated using STO-3G ab initio techniques with selected geometry optimization using the Gaussian 70 set of programs.¹⁸ Values of $S_{rr'}$ have been calculated for the interaction of carbon 2p AO's at different distances and orientations (see Figure 3) appropriate to the transition-state models represented in Figure 2. In the $[\pi 2_s + (\pi 2_s + \pi 2_s)]$ transition states the coaxially oriented p orbitals are aligned along a common axis, while the other carbon atom



Terminal coaxial overlap



Internal coaxial overlap

Figure 2. $[\pi 2_s + (\pi 2_s + \pi 2_s)]$ transition states involving terminal and internal coaxial overlap of 2p AO's.

Allene Cycloaddition Calculations

$[\pi 2_s + (\pi 2_s + \pi 2_s)]$

	d (Å)	S_{ij}	η_{ij} (=14 S_{ij})
	2.0	.2125	2.975
	2.5	.1027	1.4378

	2.0	.0697	.9758
	2.5	.0437	.6118

$(\pi 2_s + \pi 2_s)$

	2.0	.058	.7840
	2.5	.021	.2940

	2.0	.054	.7560
	2.5	.021	.2940

Figure 3. Orientations of 2p AO's and values of S_{ij} 's and η_{ij} 's.

of the dienophile is arbitrarily placed 0.65 Å out from the axis of the C=C of the allene forming an angle of ~30° between the axes of the two π systems. For the $(\pi 2_s + \pi 2_s)$ transition state a maximum value of $S_{rr'}$ is obtained at a 45° angle between the interacting π systems (see Figure 3) and this value was used in the calculations. The proportionality constant k relating $\eta_{rr'}$ to $S_{rr'}$ that has been used in these calculations is 14 as most recently used by Salem et al.^{27b}

Calculations have been carried out at separation distances (R) of 2.0 and 2.5 Å. As expected, the trends in E_{int} are the same at both distances, although being of greater magnitude at 2.0 Å. Preliminary STO-3G "supermolecule" calculations²⁹ of cycloaddition transition states for the cycloaddition of allene with ethene indicate that the separation distance at the transition state is ~2.1-2.2 Å.

Two assumptions have been made in the calculation of the E_{int} 's, the effects of which will be discussed at appropriate

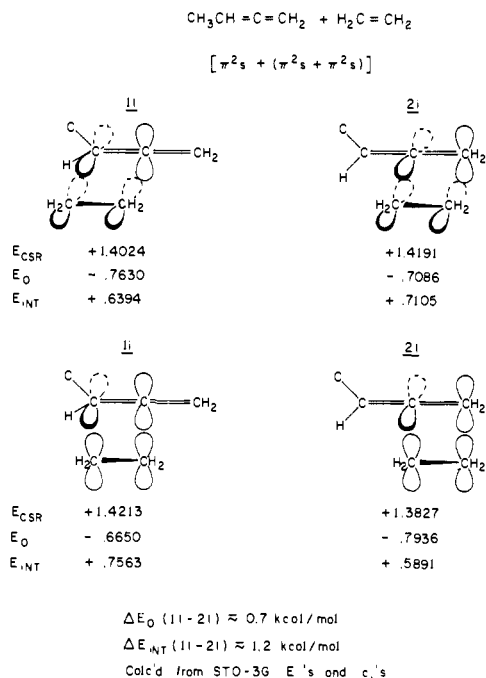


Figure 4. $[\pi^2_s + (\pi^2_s + \pi^2_s)]$ cycloaddition transition states and interaction energies for methylallene plus ethene.

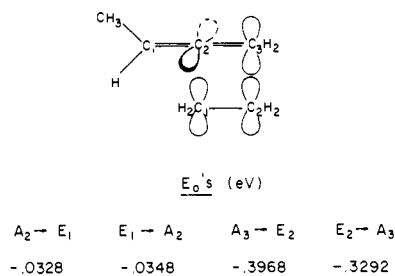


Figure 5. Contributions to E_{O} in the 2t transition state for cycloaddition of methylallene with ethene.

places. The first assumption is that the distances between the interacting atoms are the same in the transition states. The second assumption is the application of the frontier molecular orbital (FMO) approximation;³⁰ i.e., the dominant contributions to E_{1ni} arise from interactions between the π and π^* (frontier) MO's of the reactants.

Cycloaddition of Allenes with Alkenes. (a) Methylallene with Ethene. Transition states for the four possible modes of $[\pi^2_s + (\pi^2_s + \pi^2_s)]$ cycloaddition of methylallene with ethene are illustrated in Figure 4. The transition states are identified by a number representing the C=C across which the cycloaddition is occurring, and a letter i or t indicating whether the coaxial alignment of p orbitals involves the internal or terminal allene carbon. The major contributors to the E_{1ni} 's are the closed shell repulsion and the attractive overlap terms, the polar energy term being insignificant. The individual energies and the E_{1ni} 's are given in Figure 4 below the transition-state structures. The closed shell repulsion is least for transition state 2t while the attractive overlap energy is the greatest resulting in the smallest positive E_{1ni} , i.e., reflecting the lowest activation energy.³¹ Thus, cycloaddition of ethene, or any symmetrically substituted ethene such as maleic anhydride and the dialkyl fumarates and maleates, to methylallene via the $[\pi^2_s + (\pi^2_s + \pi^2_s)]$ process favors addition to the least substituted double bond by ~ 0.7 kcal/mol at 2.0 Å separation (~ 0.09 kcal/mol at 2.5 Å separation). This prediction is consistent with the chemoselectivity observed experimentally (see eq 2). (It should be noted that approach of the dienophile to the face of the

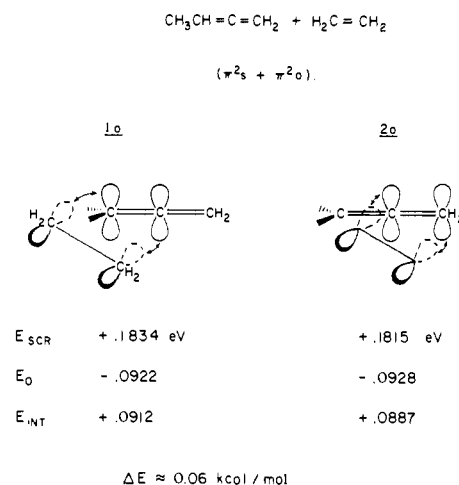


Figure 6. $(\pi^2_s + \pi^2_o)$ cycloaddition transition states and interaction energies for methylallene plus ethene.

unsubstituted double bond syn to the methyl group will experience greater steric interference than will the approach to the face anti to the methyl group, or to the two faces of the substituted double bond. Thus, the chemoselectivity observed in eq 2 is less than what would be observed in the absence of such steric effects.)

A more detailed analysis of the overlap energy contributions by the specific AO interactions is instructive. These energies are given in Figure 5 for the 2t transition state in which the designation $A_2 \rightarrow E_1$ specifies the interaction between the p AO in the HOMO on C_2 of allene (A_2) with the p AO in the LUMO on C_1 of ethene (E_1), etc. The dominant energy contributions ($\sim 91.5\%$) arise from the interactions of the coaxially aligned p orbitals. This suggests that the bond formation in the transition state is not symmetrical as assumed, but that greater bond formation occurs between the two carbon atoms whose p orbitals are coaxially aligned than between the other two carbon atoms.³² The preference for terminal over internal coaxial overlap arises from the greater value of the AO coefficients on C_3 relative to C_2 . This is a very important feature of this cycloaddition process as will be outlined later.

The results of calculations on the two modes of $(\pi^2_s + \pi^2_o)$ cycloaddition are presented in Figure 6. As expected, the magnitudes of the energies are much smaller owing to the much smaller values of $S_{rr'}$ and $\eta_{rr'}$. The overlap energy and E_{1ni} 's for cycloaddition across the two double bonds are nearly identical; $\Delta E_{1ni} \approx 0.06$ kcal/mol in favor of addition across the unsubstituted double bond.

The smaller values of the E_{1ni} 's for the $(\pi^2_s + \pi^2_o)$ processes relative to those for the $[\pi^2_s + (\pi^2_s + \pi^2_s)]$ processes might lead one to predict that reactivity via the former is greater. These results, however, arise from the simplifying assumptions inherent in the FMO approximation and are not at all consistent with preliminary "supermolecule" STO-3G calculations in which interactions between all AO's in all MO's on the carbon atoms of the two π systems are included.²⁹ Such calculations for selected geometries of the allene-ethene "supermolecule" indicate that the $[\pi^2_s + (\pi^2_s + \pi^2_s)]$ process is of considerably lower energy, ~ 25 kcal/mol at 2.1-Å separation.²⁹ Although E_{overlap} 's and E_{1ni} 's provide a means of distinguishing between possible modes of cycloaddition of the same mechanistic type, comparisons between different mechanistic processes are best made on the basis of chemo- and regioselectivities.

A comparison of the chemoselectivities predicted for the two different cycloaddition mechanistic possibilities with that observed experimentally (eq 2) suggests that the cycloaddition of methylallene with a dienophile occurs via the $[\pi^2_s + (\pi^2_s + \pi^2_s)]$ process.

[$\pi^2_s + (\pi^2_s + \pi^2_s)$]			[$\pi^2_s + (\pi^2_s + \pi^2_s)$]				
Mode	E_o (eV)	Product	Mode	E_o (eV)	E_p (eV)	$E_o + E_p$ (eV)	Product
<u>11</u>	- .7308		11HT	- .4923	+ .0068	- .4855	
<u>1i</u>	- .6541	<u>11</u>	11HT	- .5102	+ .0068	- .5034	<u>13</u>
<u>2i</u>	- .7106		11HH	- .5808	+ .0050	- .5758	
<u>2t</u>	- .7868	<u>12</u>	1iHH	- .4731	+ .0050	- .4681	<u>14</u>
			2iHT	- .4849	+ .0675	- .4174	
	($\pi^2_s + \pi^2_o$)		2iHT	- .6270	+ .0675	- .5595	<u>15</u>
<u>1</u>	- .0905	<u>11</u>	2iHH	- .5552	+ .1111	- .4441	
<u>2</u>	- .0903	<u>12</u>	2iHH	- .4898	+ .1111	- .3787	<u>16</u>
					($\pi^2_s + \pi^2_s$)		
			1HT	- .0681	+ .0068	- .0613	<u>13</u>
			1HH	- .0667	+ .0050	- .0617	<u>14</u>
			2HT	- .0675	+ .0675	.0000	<u>15</u>
			2HH	- .0647	+ .1111	+ .0464	<u>16</u>

Figure 7. Overlap energies and structures derived from the cycloaddition of 1,1-dimethylallene with ethene. In the transition state designations the number indicates the C=C across which cycloaddition is occurring and the letters i and t indicate internal and terminal coaxial overlap, respectively.

(b) **1,1-Dimethylallene with Ethene.** Overlap energies, E_o 's, for the various modes of cycloaddition of 1,1-dimethylallene with ethene are presented in Figure 7. Of the [$\pi^2_s + (\pi^2_s + \pi^2_s)$] processes, 2t to produce **12** is favored over 1t by ~ 2.6 kcal/mol at 2.0 Å and ~ 0.65 kcal/mol at 2.5 Å separation. The greater chemoselectivity predicted with 1,1-dimethylallene relative to methylallene is due to the higher values of the AO coefficients at C₃ (at the expense of the AO coefficients on C₂) in the dimethylallene. In contrast, cycloaddition across the substituted double bond is very slightly favored in the ($\pi^2_s + \pi^2_o$) process.

Cycloaddition of 1,1-dimethylallene with maleic anhydride occurs exclusively "across" the unsubstituted double bond (eq 3), while with dimethyl fumarate addition "across" the unsubstituted double bond is highly favored. This is despite the presence of the two methyl groups which sterically impede attack at both faces of the remote double bond. Thus, the observed results are consistent only with the operation of the highly chemoselective [$\pi^2_s + (\pi^2_s + \pi^2_s)$] mechanism.

(c) **1,1-Dimethylallene with Acrylonitrile.** Application of the theory to the cycloaddition of 1,1-dimethylallene with an unsymmetrical, polar dienophile, such as acrylonitrile, provides an opportunity to distinguish between different regioselectivities within each reagent, and the effect of the polar energy contribution. Figure 8 summarizes the results. The mode of [$\pi^2_s + (\pi^2_s + \pi^2_s)$] cycloaddition is designated by a number indicating the double bond across which cycloaddition occurs, i or t indicating whether coaxial alignment of the p AO's involves an internal or terminal carbon of the allene, with HT and HH designating head-to-tail or head-to-head 1,1-dimethylallene-acrylonitrile orientation. For the modes of ($\pi^2_s + \pi^2_s$) cycloaddition identical designations apply. If one considers only the overlap energy term, E_o , formation of **15** is favored over **14** by ~ 1.1 kcal/mol at 2.0 Å (0.26 kcal/mol at 2.5 Å). This chemo- and regioselectivity is the same as that observed experimentally.³³

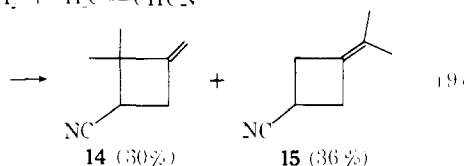


Figure 8. Interaction energies and structures derived from the various possible modes of cycloaddition of 1,1-dimethylallene with acrylonitrile. See the text for the definition of the mode of the cycloaddition.

If the polar energy term (E_p) is added in, the predicted product distribution of **14** and **15** is reversed by ~ 0.4 kcal/mol. It is necessary to point out, however, that E_p is calculated on the basis of the total charge on the atoms which is a function of the occupancy of all OMO's and not just the occupancy of the π OMO's as assumed in the FMO approximation.³⁴ The total contribution of E_p to E_{Jn1} in eq 8 is that given in Figure 8, but the value of E_o will increase in a relative manner on inclusion of the E_o 's between the lower energy OMO's and higher energy UMO's. Thus, in the energy values cited in Figure 8 greater attention must be focused on the values of E_o . Even within these restrictions, it is remarkable how the application of second-order PMO theory in this section, as well as in later sections, on the [$\pi^2_s + (\pi^2_s + \pi^2_s)$] and the ($\pi^2_s + \pi^2_o$) cycloaddition processes results in a correlation of experimental product regio- and chemoselectivity most consistent with the former process.

(d) **1,3-Dimethylallene with Acrylonitrile.** The most favorable mode of cycloaddition of 1,3-dimethylallene with acrylonitrile is predicted to be the [$\pi^2_s + (\pi^2_s + \pi^2_s)$] process involving coaxial overlap at the terminal allene carbons to give the observed products of gross structures **6** and **7** (eq 1). Coaxial overlap at the terminal carbons is favored over coaxial overlap at the internal allene carbon by ~ 1.7 kcal/mol, and over formation of the regioisomer by ~ 0.9 kcal/mol.

Cyclodimerization of Allenes. Transition state designations used in defining the various modes of cyclodimerization of allenes discussed in the following sections are as follows.

(1) The first number designates the double bond "across" which cycloaddition occurs in the ($\pi^2_s + \pi^2_s$) component (indicated in each of the appropriate figures).

(2) The letters i and t indicate coaxial overlap of the AO at the internal or terminal carbon of the allene in the ($\pi^2_s + \pi^2_s$) component [not applicable in the ($\pi^2_s + \pi^2_o$) processes].

(3) The second number designates the number of the double bond involved in the π^2_s component.

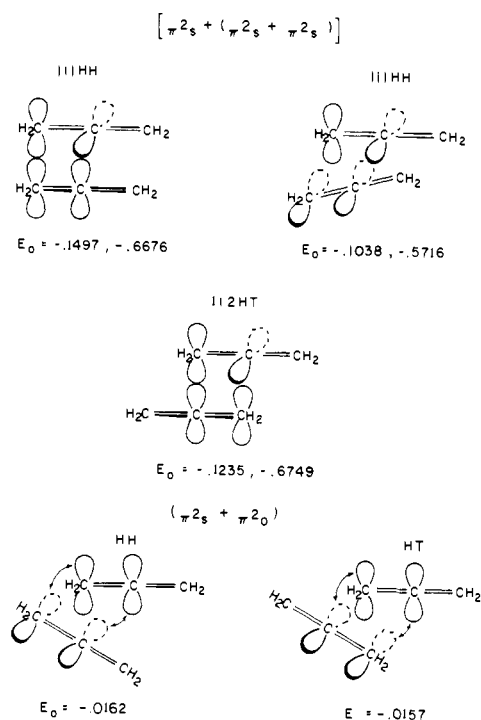


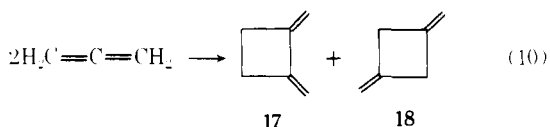
Figure 9. Overlap energies and transition states for the various modes of cyclodimerization of allene. See the text for the definition of transition state designations. The first energy (eV) is calculated from 4-31G calculations of c_i and E and the second from STO-3G calculations. For the $(\pi 2_s + \pi 2_u)$ the E_0 's are calculated from 4-31G results.

(4) The letters HH and HT represent head-to-head and head-to-tail orientations of the $(\pi 2_s + \pi 2_s)$ and $\pi 2_s$ components, respectively.

All energy values in the figures are for a separation distance of 2.0 Å.

(a) Cyclodimerization of Allene. Transition states and E_0 's for the $[\pi 2_s + (\pi 2_s + \pi 2_s)]$ and $(\pi 2_s + \pi 2_u)$ cyclodimerizations of allene are given in Figure 9. In the former process, calculations using STO-3G coefficients and energies suggest that transition state 1t2HT is very slightly favored over 1t1HH,³⁵ whereas calculations using 4-31G derived c_i 's and energies favor 1t1HH by ~ 0.6 kcal/mol.³⁶ Both sets of calculations, however, indicate that in the formation of **17**, coaxial overlap at the terminal allene carbon atoms, is highly favored over coaxial overlap at the internal allene carbon atoms (~ 2.2 and ~ 1.1 kcal/mol at the STO-3G and 4-31G levels, respectively).³⁷

In the $(\pi 2_s * \pi 2_u)$ process, the STO-3G-based calculations slightly favor the formation **18**, while the 4-31G-based calculations indicate **17** and **18** are essentially equally favored.

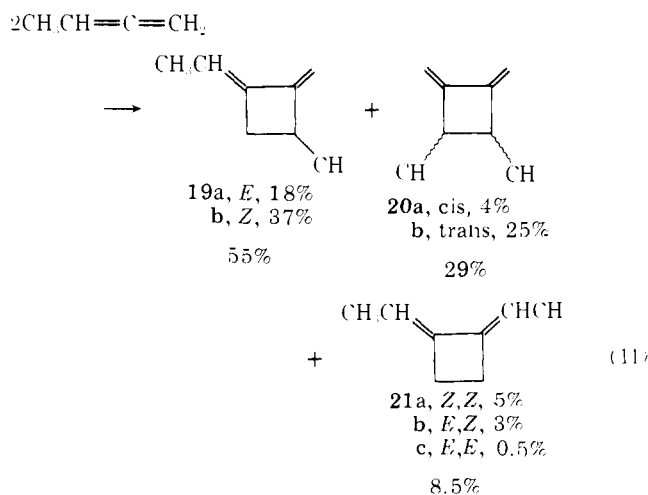


(b) Cyclodimerization of Methylallene. On the basis of E_0 , cyclodimerization via the $[\pi 2_s + (\pi 2_s + \pi 2_s)]$ process favors formation of **21** > **19** > **20** (the formation of the other possible isomeric structures is still less favorable), whereas in the $(\pi 2_s + \pi 2_u)$ process all adducts are predicted to be formed in comparable quantities. Inclusion of E_p reduces the favorability of formation of **21** and **19** resulting in a predicted product distribution **19** ~ **20** > **21**.

Experimentally the cyclodimerization of methylallene produces the mixture of cycloadducts shown in eq 11 in which the relative yields of the stereoisomers is **19** > **20** > **21**.²⁰

Mode	E_0	E_p	E_{int}	Product
$[\pi 2_s + (\pi 2_s + \pi 2_s)]$				
2t2HH	<u>-0.7424</u>	+0.2066	-0.5358	(22)
2t2HH	-0.5715	+0.2066	-0.3649	22
2t2HT	-0.6329	+0.0056	-0.6273	(23)
2t2HT	-0.6785	+0.0056	-0.6729	23
2t1HH	-0.6743	+0.0030	-0.6713	(24)
2t1HH	-0.6362	+0.0030	-0.6332	24
1t1HH	-0.6512	+0.0006	-0.6506	(25)
1t1HH	-0.5616	+0.0006	-0.5610	25
2t1HT	<u>-0.7018</u>	+0.0111	-0.6907	(26)
2t1HT	-0.6107	+0.0111	-0.5996	26
1t1HT	-0.6269	+0.0003	-0.6266	(27)
1t1HT	-0.5868	+0.0003	-0.5865	27
$(\pi 2_s + \pi 2_0)$				
22HH	<u>-0.0810</u>	+0.2067	+0.1257	22
22HT	-0.0803	+0.0056	-0.0747	23
2t1HH	-0.0807	+0.0017	-0.0790	24
2t1HT	-0.0807	+0.0111	-0.0696	25
1t1HH	<u>-0.0808</u>	+0.0006	-0.0802	26
1t1HT	-0.0807	+0.0003	-0.0804	27

Figure 10. Interaction energies and products of the various modes of cyclodimerization of 1,1-dimethylallene. The underlined values indicate the most favorable (—) and the second best (---) processes.



(c) Cyclodimerization of 1,1-Dimethylallene (3). Based on E_0 's the major products predicted to be formed in the 6- π electron cycloaddition process are **22** > **26** (by ~ 0.9 kcal/mol) (Figure 10), both products being formed via transition states having coaxial overlap at the terminal allene carbon atoms. This prediction compares remarkably well with that observed experimentally (eq 5),²⁴ despite the apparent steric crowding between the two "inside" methyl groups on the incipient diene

Mode	E_o	E_p	E_{int}	Product
	$[\pi 2_s + (\pi 2_s + \pi 2_s)]$			
2t2HH	<u>-7329</u>	+1195	-6134	 (28)
2:2HH	-5976	+1195	-4781	 (29)
2t2HT	-6373	+0852	-5521	 (29)
2:2HT	<u>-6880</u>	+0852	-6028	 (30)
2t1HH	-6838	-0456	-7294	 (30)
2:1HH	-5941	-0456	-6397	 (30)
1t1HH	-5049	+4532	-0517	 (31)
1:1HH	-5732	+4532	-1200	 (31)
2t1HT	-6275	-1924	-8199	 (32)
2:1HT	-6341	-1924	<u>-8265</u>	 (32)
1t1HT	-5083	-0882	-5964	 (33)
1:1HT	-5735	-0882	-6617	 (33)
	$(\pi 2_s + \pi 2_o)$			
22HH	-0814	+1195	+0381	 (28)
22HT	-0808	+0851	+0043	 (29)
2t1HH	-0788	-0456	-1244	 (30)
2t1HT	-0796	-1925	<u>-2721</u>	 (31)
1t1HH	-0721	+4532	+3811	 (32)
1t1HT	-0746	-1763	-2509	 (33)

Figure 11. Interaction energies and products of the various modes of cycloaddition and cyclodimerization of 1,1-difluoroallene. The underlined values indicate the most favorable processes.

system in the transition state. Inclusion of the E_p term leads to a substantial reduction in the E_{int} of the 2t2HH process thus favoring formation of **26**. As pointed out earlier the effect of E_p on product distribution will be less than that calculated in this study on the basis of the assumptions made and thus **22** should be favored.

The values of E_o for the $(\pi 2_s + \pi 2_o)$ processes are all very nearly equal. Inclusion of E_p results in a prediction that **27** and **26** should be the major products. In this case, even a substantial reduction in E_p for the formation of **22** would still not make the formation of **22** competitive with the formation of **27**.

The results of the calculations on the cyclodimerization of **3** are clearly more consistent with the $[\pi 2_s + (\pi 2_s + \pi 2_s)]$ concerted process.

(d) Cyclodimerization of 1,1-Difluoroallene. On the basis of E_o **28** is favored in the $[\pi 2_s + (\pi 2_s + \pi 2_s)]$ cyclodimerization of 1,1-difluoroallene (by ~ 1.0 kcal/mol), whereas inclusion of E_p favors the formation of **32** (by ~ 2.2 kcal/mol) (see Figure 11). Even if one acknowledges that the values of the E_p 's are substantially overestimated relative to the E_o 's, reduction of the E_p 's to 40% of their values in Figure 11 still leads to the prediction that **32** should be the major product formed! Experimentally, **32** is reported to be the sole cycloadduct formed.²⁵ In the case of the highly polar 1,1-difluoroallene the E_p term appears to determine the regioselectivity of cyclodimerization. **31** is favored in the $(\pi 2_s + \pi 2_o)$ process.

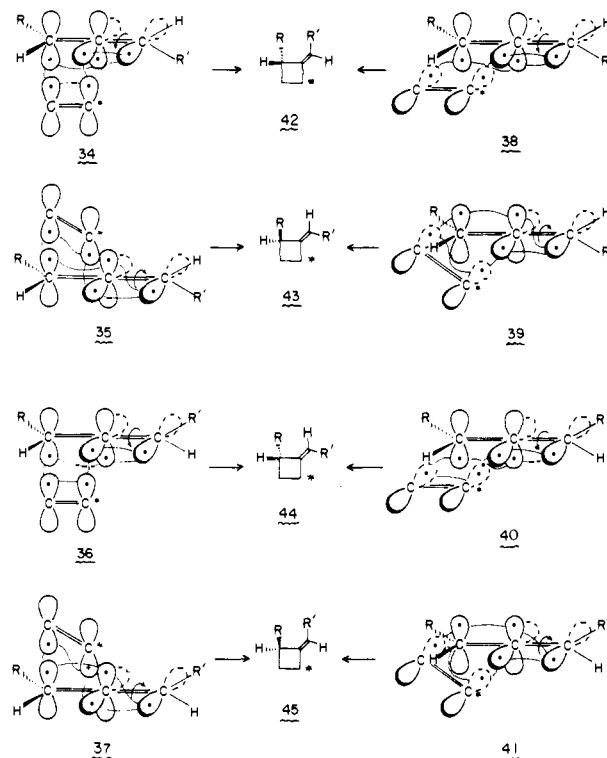


Figure 12. Illustration of the stereochemical control in product formation in the $[\pi 2_s + (\pi 2_s + \pi 2_s)]$ transition states.

It is interesting to note that the $[\pi 2_s + (\pi 2_s + \pi 2_s)]$ process favored when E_p is included involves coaxial overlap at the internal allene carbon atom.

Stereochemical Considerations. In the foregoing sections second-order PMO theory was used to predict chemo- and regioselectivities in cycloaddition and cyclodimerization of allenes in an attempt to distinguish between the possible $[\pi 2_s + (\pi 2_s + \pi 2_s)]$ and $(\pi 2_s + \pi 2_o)$ modes of reaction. In all cases the chemo- and regioselectivity predicted by the former process corresponded more closely to experimental observations. In this section the stereochemical features of the two processes are discussed and compared with reported results.

Figure 12 illustrates the various terminal and internal coaxial overlap transition states for the $[\pi 2_s + (\pi 2_s + \pi 2_s)]$ cycloaddition of a dienophile with the two enantiomers of a 1,3-disubstituted allene. In these transition states it is important to note that the direction of rotation of the terminal CHR is determined by the direction of approach of the dienophile and the resultant orbital interactions necessary to achieve an aromatic transition state.³⁸ (It should be pointed out that for each of the transition states shown in Figure 12, there exists complementary transition states involving bonding to the backside lobe of p AO on the central allene carbon. These complementary transition states, however, result in the formation of the same product.) In the pairs of transition states **34** and **35** and **36** and **37**, approach of the dienophile is more sterically hindered in **34** and **37** due to interaction between R' and the group on C^* pointing toward R' , thus favoring formation of **43** and **44**. In contrast, the steric interactions are essentially the same in transition states **38**–**41** suggesting that all four products should be formed. (The complementary transition states with rearward approach of the dienophile are more sterically congested and their contribution to product formation will be less, but also essentially the same.)

In the $(\pi 2_s + \pi 2_o)$ process (Figure 13) the stereochemistry about the exocyclic double bond is determined only by the orientation of approach of the dienophile. The least sterically

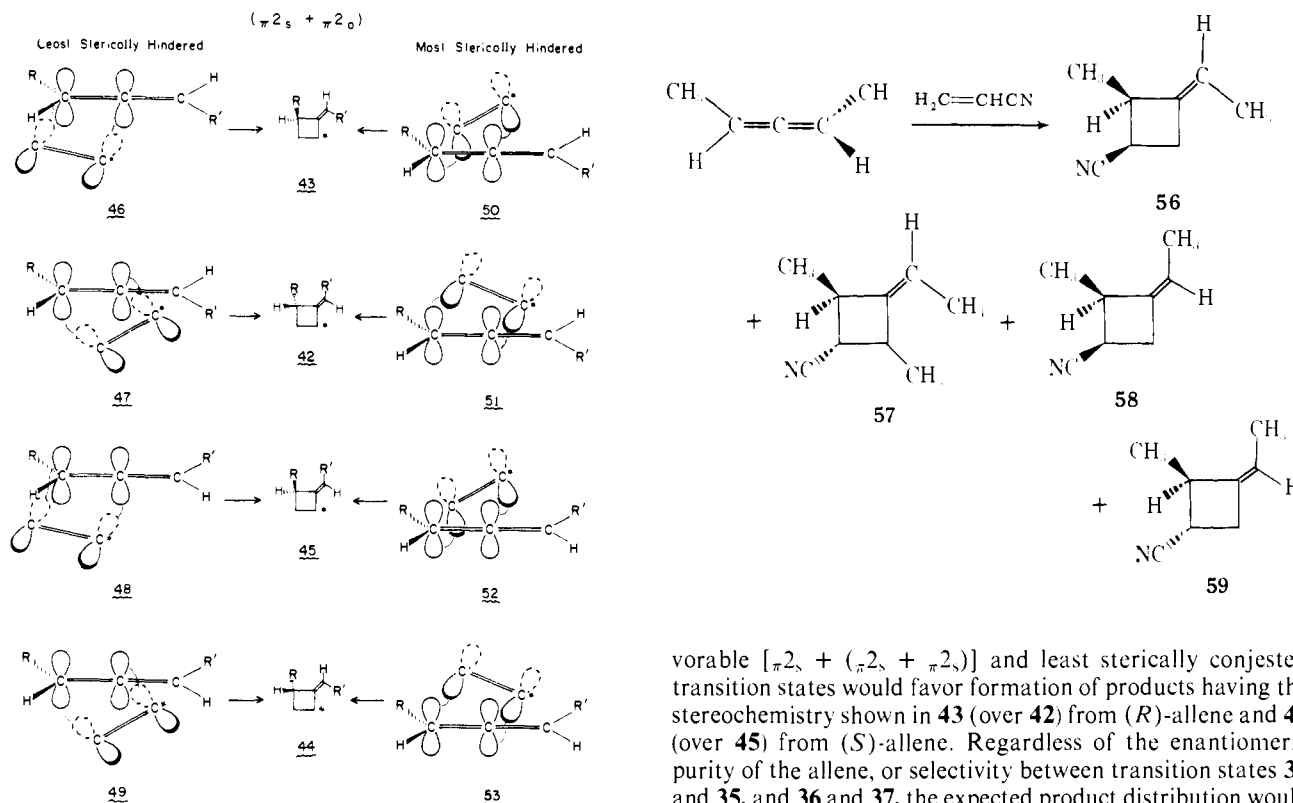
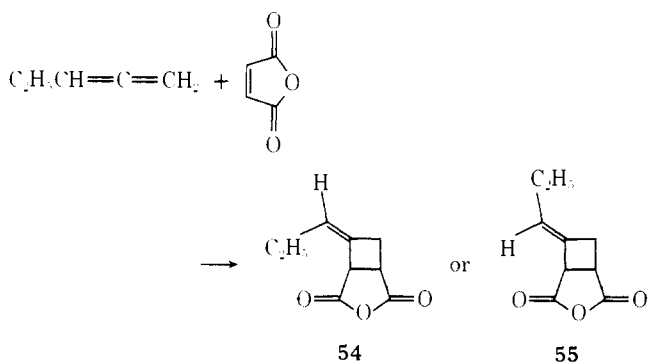


Figure 13. Illustration of the stereochemical control in product formation in the $(\pi^*2_s + \pi^*2_o)$ transition states.

hindered transition states **46–49** involve approximately the same steric interactions and, thus, should result in the formation of all four products in comparable quantities. Transition states **50–53** are all more, but equally, sterically congested and will contribute less toward product formation.

In the following sections comparisons of the predictions of the various models will be made with experimental observations.

(a) **Cycloaddition Reactions of Allenes.** The stereochemistry about the exocyclic double bond in the product from cycloaddition of a monosubstituted allene, for example, as in **9** in eq 2, has not been determined. If the cycloaddition occurs as predicted by second-order PMO theory, transition state **35** ($R = H$) will be favored over **34** favoring formation of **54** over **55**. Should cycloaddition occur via transition states **38** ($R =$



H) or **39**, or **46** or **47**, the major product expected would be **55**.

The cycloaddition of optically active 1,3-dimethylallene (enantiomeric excess of the (R) isomer) with acrylonitrile¹¹ produces the four optically active adducts **56–59**, all possessing the (R) configuration at C_2 .³⁹ Cycloaddition via the most fa-

vorable $[\pi 2_s + (\pi 2_s + \pi 2_o)]$ and least sterically congested transition states would favor formation of products having the stereochemistry shown in **43** (over **42**) from (R) -allene and **44** (over **45**) from (S) -allene. Regardless of the enantiomeric purity of the allene, or selectivity between transition states **34** and **35**, and **36** and **37**, the expected product distribution would be **43** > **44** > **42** > **45** if product is formed only via that single process. In contrast, if products are formed only via transition states **38–41**, a product distribution of **42** > **43** > **45** > **44** is predicted; however, long-range steric effects do not appear to be as severe in **34–37** and less discrimination might be expected.

Adducts **56** and **57** correspond in stereochemistry to **43**, while **58** and **59** correspond to **45**. If a single concerted mechanistic process is operative, the stereochemical distribution of the products cannot be accounted for. However, should product formation from transition states **38–41** contribute to that via **34–37**, a product distribution of **43** > **44** and **45** > **42** is possible which would result in the observed stereospecificity.^{40,41} The only *single path mechanism* which fully accounts for the observed stereochemistry of the cycloaddition is that originally proposed by Baldwin and Roy¹¹ involving restricted formation and collapse of an intermediate diradical.

(b) **Cyclodimerization of Allenes.** The transition states in Figures 12 and 13 can be elaborated for the cyclodimerization of allenes by attaching a $=CH_2$ to the asterisked carbon of the dienophile. With substituted allenes the number of individual transition states markedly increases due to different orientations of the substituent(s) on one allene with respect to the substituent(s) on the other allene, and analysis of the possible steric interactions which will favor one transition state structure over other isomeric transition state structures becomes more difficult. Whereas in the cycloaddition reaction the only steric effect that appears to be important is that between a group on C^* of the dienophile and R' on the allene (see Figure 12), in the cyclodimerization of allenes three steric effects are operative: (1) between groups attached to the carbon atoms of the 3–4 bond in the product; (2) between functions attached to the carbon atoms of the penultimate exocyclic methylene groups; and (3) between the π systems of each allene with substituents on the other allene (π – π interactions are considered to be the same in all transition states). The dominant interaction appears to be (1), while of (2) and (3). (3) appears to be more important (see Figure 14).

(c) **Cyclodimerization of Methylallene.** The cyclodimerization of a monosubstituted allene such as methylallene best il-

illustrates the effects outlined immediately above on the stereochemistry of product formation.

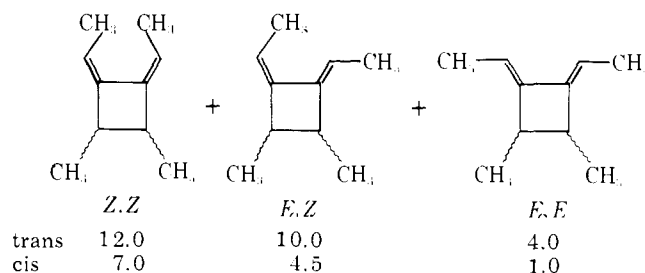
In the formation of **20a** via the 1t1HH-type transition state **60a** (Figure 14), the methyl groups are nearly eclipsed (dihedral angle $\sim 15^\circ$), whereas in the formation of **20b** via **60b** the nearly eclipsed groups are hydrogen with methyl (Figure 14). Thus, quite clearly, **60b** is of lower energy and favors formation of the trans adduct **20b** over the cis adduct **20a**. This is consistent with that observed experimentally (eq 11).

Formation of **19a** and **19b** occurs via the 2t1HT transition states **61a** and **61b**. In **61a** there are long-range H-CH₃ interactions and π -H and severe π -CH₃ interactions (indicated by the arrows). As **61b** is less sterically congested, formation of the *more* sterically congested **19b** is favored. This is again consistent with experimental observations.

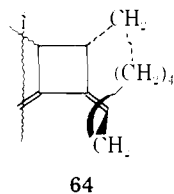
Analysis of the formation of **21a-c** is more complex. Four 2t2HH transition states are possible. Analysis of models of the transition states as described above indicates that the steric congestion increases in the sequence **62a** > **62b** > **62c** > **62d**. This predicts a product distribution **21b** > **21a** > **21c**; i.e., the major products are the most sterically congested! This prediction corresponds amazingly well with that observed experimentally (eq 11).

(d) **Cyclodimerization of 1,3-Disubstituted Allenes.** The stereochemical analysis of the cyclodimerization of a 1,3-disubstituted allene involves the comparison of eight transition states for each individual mode of cyclodimerization of *d* with *d* and of *d* with *l*. Two such systems have been studied experimentally, racemic and optically active 1,3-dimethylallene²² and 1,2-cyclononadiene.²¹

In the cyclodimerization of 1,3-dimethylallene a combination of all three steric effects noted in the previous section is encountered. The resulting trends predicted are: trans > cis relationship of the ring methyls in each series, and *E,Z* > *Z,Z* > *E,E*. Again the predicted product distribution is amazingly similar with that observed (relative yields are given).⁴¹



The stereochemical analysis of the cyclodimerization of 1,2-cyclononadiene (**63**) is considerably simplified by immediate rejection from consideration transition states in which the connecting chain of methylenes penetrates the other allene, and by rejection of processes resulting in the formation of products with the impossible stereochemistry shown in **64**.



Analysis of models of transition states for cyclodimerization of *d*- with *d*-**63** involving terminal coaxial overlap indicates that **65** should be the major product formed, with **68** possibly being formed in minor amounts. Very interestingly, cyclodimerization involving internal coaxial overlap is predicted to result in the formation of only **65**. However, internal coaxial overlap transition states are more sterically congested relative

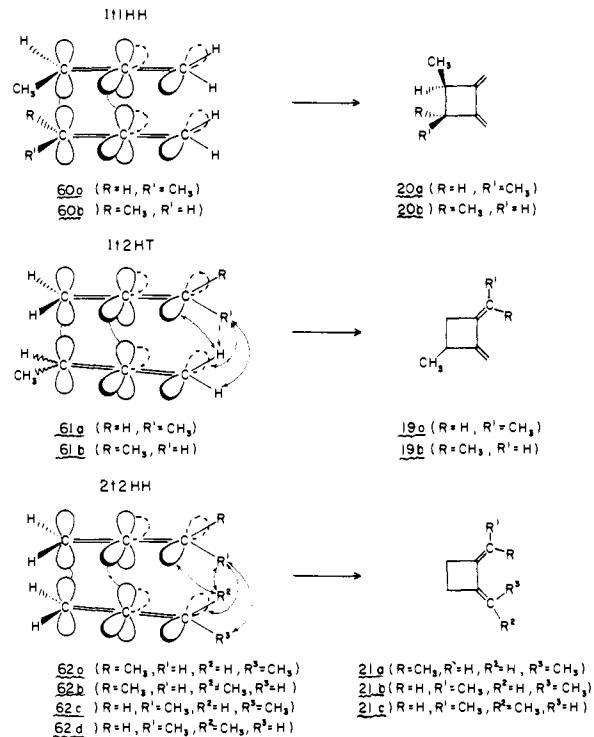
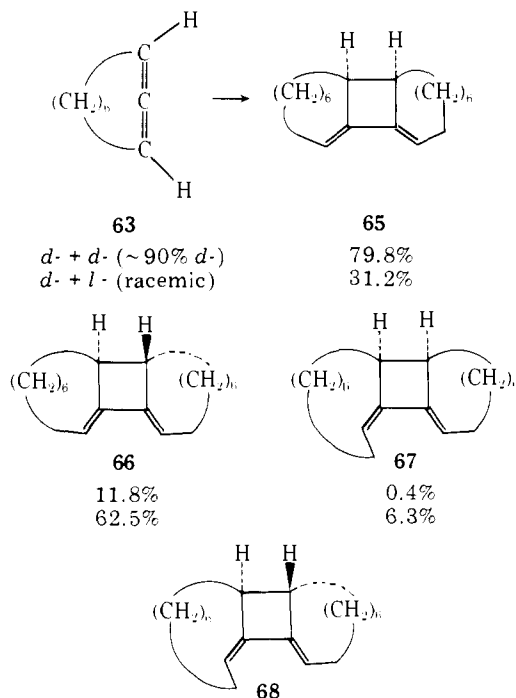


Figure 14. Illustration of the stereochemical control of product formation in the cyclodimerization of methylallene via the 1t1HH, 1t2HT, and 2t2HH transition states.

to those involving terminal coaxial overlap. Cyclodimerization of *d*- with *l*-**63** is predicted to result in the formation of only **66** and **67** (the former being preferred) via transition states involving either terminal or internal coaxial overlap. With the exception of the predicted possible formation of **68**, the predictions are fully consistent with the experimental results.



Comment on the H-D Kinetic Isotope Effects in the [$\pi 2_s + \pi 2_s$] Process. In the presently proposed concerted mechanism for cycloaddition with an allene there are three types of secondary kinetic isotope effects: one arising from the change in hybridization at the carbons undergoing σ -bond

formation, one arising from the rotation (C-H bending) of the methylene group, and one arising from changes in the MO structure at the methylene group affecting the C-H stretching and bending deformations. The extent of the contribution of each of these will depend on the relative extents of bond formation and rotation of the methylene group which need not be the same. There is currently no adequate experimental data available which allow for an estimation of the magnitude of the last two isotope effects. Experimental and theoretical studies are currently under way in our laboratories to evaluate these effects.

Acknowledgments. The author gratefully acknowledges support of this research by a NATO Senior Fellowship in Science administered by the National Science Foundation, by a National Science Foundation research grant (CHE77-08627), and by the Computing Center of the University of Notre Dame. The author also wishes to thank Professor J.-M. Lehn for the hospitality extended during his NATO fellowship tenure at the Université Louis Pasteur de Strasbourg, Strasbourg, France.

References and Notes

- (1) D. J. Pasto and A. F.-T. Chen, *J. Am. Chem. Soc.*, **93**, 2562 (1971); D. J. Pasto, A. F.-T. Chen, and G. Binsch, *ibid.*, **95**, 1553 (1973).
- (2) D. J. Pasto and J. K. Borchardt, *J. Am. Chem. Soc.*, **96**, 6944 (1974).
- (3) D. J. Pasto, J. K. Borchardt, T. P. Fehlner, H. F. Baney, and M. E. Schwartz, *J. Am. Chem. Soc.*, **98**, 526 (1976).
- (4) D. J. Pasto, A. F.-T. Chen, G. Ciurdaru, and L. A. Paquette, *J. Org. Chem.*, **38**, 1015 (1973); D. J. Pasto and J. K. Borchardt, *J. Am. Chem. Soc.*, **96**, 6937 (1974).
- (5) D. J. Pasto and D. Wampfler, *Tetrahedron Lett.*, 1933 (1974).
- (6) D. J. Pasto and A. F.-T. Chen, *Tetrahedron Lett.*, 2995 (1972).
- (7) D. J. Pasto and A. F.-T. Chen, *Tetrahedron Lett.*, 713 (1973).
- (8) D. J. Pasto, T. P. Fehlner, M. E. Schwartz, and H. F. Baney, *J. Am. Chem. Soc.*, **98**, 530 (1976).
- (9) H. E. Zimmerman, *Acc. Chem. Res.*, **4**, 272 (1971).
- (10) E. F. Kiefer and M. Y. Okamura, *J. Am. Chem. Soc.*, **90**, 4187 (1968).
- (11) J. E. Baldwin and U. V. Roy, *J. Chem. Soc. D*, 1225 (1969).
- (12) K. Alder and O. Ackermann, *Chem. Ber.*, **90**, 1697 (1957).
- (13) S. H. Dai and W. R. Dolbier, Jr., *J. Am. Chem. Soc.*, **94**, 3946 (1972); W. R. Dolbier, Jr., and S. H. Dai, *ibid.*, **90**, 5028 (1968).
- (14) L. H. Sutcliffe and A. D. Walsh, *J. Chem. Soc.*, 849 (1952).
- (15) P. G. Wilkinson and R. S. Mulliken, *J. Chem. Phys.*, **23**, 1895 (1955).
- (16) F. Brogli, J. K. Crandall, E. Heilbronner, E. Kloster-Jensen, and S. A. Sojka, *J. Electron. Spectrosc. Relat. Phenom.*, **2**, 455 (1973).
- (17) Cf. C. Baker and D. W. Turner, *J. Chem. Soc. D*, 480 (1969).
- (18) W. J. Hehre, R. F. Stewart, and J. A. Pople, *J. Chem. Phys.*, **51**, 2657 (1969); R. Ditchfield, W. J. Hehre, and J. A. Pople, *J. Chem. Phys.*, **54**, 724 (1971).
- (19) 4-31G calculations were carried out on STO-3G geometry optimized structures.
- (20) J. J. Gajewski and C. N. Shih, *J. Am. Chem. Soc.*, **91**, 5900 (1969).
- (21) W. R. Moore, R. D. Bach, and T. M. Ozretich, *J. Am. Chem. Soc.*, **91**, 5918 (1969).
- (22) J. J. Gajewski and W. A. Black, *Tetrahedron Lett.*, 899 (1970).
- (23) T. L. Jacobs, J. R. McClenon, and O. J. Musico, Jr., *J. Am. Chem. Soc.*, **91**, 6038 (1969).
- (24) J. R. McClenon, Ph.D. Thesis, University of California at Los Angeles; *Diss. Abstr.*, **25**, 101 (1964).
- (25) W. H. Knoch and D. D. Coffman, *J. Am. Chem. Soc.*, **82**, 3873 (1960).
- (26) C. W. N. Crumper, Z. T. Formum, P. M. Greaves, and S. R. Landor, *J. Chem. Soc., Perkin Trans 2*, 885 (1973).
- (27) (a) L. Salem, *J. Am. Chem. Soc.*, **90**, 543, 553 (1968); (b) A. Devaquet and L. Salem, *ibid.*, **91**, 3793 (1969).
- (28) This mechanistic possibility has been mentioned only briefly in a footnote of ref 23.
- (29) D. J. Pasto, results of unpublished preliminary STO-3G calculations.
- (30) J. Fukui, *Acc. Chem. Res.*, **4**, 57 (1971), and references cited therein.
- (31) The same trend in relative energies is derived using 4-31G orbital energies and outer, or diffuse, orbital coefficients.
- (32) STO-3G "supermolecule" calculations on the allene-ethene system are in accord with this notion.
- (33) H. N. Cripps, J. K. Williams, and W. H. Sharkey, *J. Am. Chem. Soc.*, **81**, 2723 (1959).
- (34) The calculated dipole moments of methylallene [0.311 (STO-3G) and 0.365 D (4-31G)] and acrylonitrile (3.229 D) are in reasonable agreement with the experimental values of 0.403 and 3.87 D, respectively.
- (35) In the STO-3G calculations on allene the degenerate HOMO's and the LUMO's are extensively mixed whereas in the 4-31G calculations this mixing is less extensive.
- (36) The preference for forming the conjugated 1,2-dimethylenecyclobutanes in the cyclodimerization of allenes has previously been attributed to the formation of the more stable, conjugated diene system (ref 37).
- (37) D. R. Taylor, *Chem. Rev.*, **67**, 317 (1967).
- (38) The direction of rotation required to achieve a Huckel aromatic transition state also results in the generation of symmetry-adapted MO's of the butadiene system (Ψ_1 or Ψ_2), whereas rotation in the other direction does not.
- (39) The optical purity of the 1,3-dimethylallene and the optical purity and ratio of the products **56-59** were not reported (ref 11).
- (40) A product distribution of **43 > 44 > 45 > 42** can be derived with a selectivity of 70:30 between the [$\pi_2s + (\pi_2s + \pi_2s)$] and [$\pi_2s + \pi_2s$] processes and selectivities of 80:20 between **35 > 34** and 70:30 between **38 > 39**.
- (41) In the case of the cyclodimerization of partially resolved 1,3-dimethylallene, the optical purity of the allene was ~15%. As a result the product distributions derived from racemic and the partially resolved allene are very similar.

Theoretical Evidence for Nonplanar Cyclopropylcarbiniyl Cations. Effect of Orbital Distortion on Endo and Exo Solvolytic Product Ratios

Robert D. Bach* and Paul E. Blanchette

Contribution from the Department of Chemistry, Wayne State University, Detroit, Michigan 48202. Received April 5, 1978

Abstract: Theoretical evidence based upon ab initio molecular orbital calculations is described which provides an explanation for the predominant formation of endo tricyclic solvolytic products derived from the tricyclo[3.3.0.0^{2,8}]octan-3-yl cation and related carbenium ions. A theoretical rationale is presented which invokes angular distortion and a nonplanar cationic center in the carbenium ion intermediate. The above arguments are based upon a comparison of the relative energies involved in the calculated rotational barrier and sp^2 to sp^3 rehybridization of methylcyclopropylcarbiniyl cation.

Introduction

Early evidence for the planarity of carbenium ions was based upon solvolysis studies of optically active substances which led to racemic products.^{1,2} Strongly suppressed rates of carbenium ion formation at a bridgehead have also been cited

as evidence for the planarity of carbocations. More recently, Raman, infrared,^{3a} and ¹³C nuclear resonance studies^{3b} have provided direct evidence for the planarity of the ⁺CC₃ carbon skeleton. Theoretical investigations have also demonstrated the planarity or near planarity of carbenium ion intermediates in the absence of solvent or symmetry influences. For example,